Journal of Alloys and Compounds 509 (2011) 7060–7065

Contents lists available at ScienceDirect

Journal of Alloys and Compounds

journal homepage: www.elsevier.com/locate/jallcom

Effect of C particle size on the mechanism of self-propagation high-temperature synthesis in the Ni–Ti–C system

Y.F. Yang[a,*], H.Y. Wang[b], J.G. Wang[b], Q.C. Jiang[b,*]

[a] The University of Queensland, School of Mechanical and Mining Engineering, ARC Centre of Excellence for Design in Light Metals, Brisbane, QLD 4072, Australia
[b] Key Laboratory of Automobile Materials of Ministry of Education, Department of Materials Science and Engineering, Jilin University, Nanling Campus, Changchun 130025, PR China

ARTICLE INFO

Article history:
Received 22 February 2011
Received in revised form 25 March 2011
Accepted 30 March 2011
Available online 5 April 2011

Keywords:
Ceramics
Powder metallurgy
Composites materials
Chemical synthesis
Phase transitions

ABSTRACT

Effect of C particle size on the mechanism of self-propagation high-temperature synthesis (SHS) in the Ni–Ti–C system was investigated. Fine C particle resulted in a traditional mechanism of dissolution-precipitation while coarse C particle made the reaction be controlled by a mechanism of the diffusion of C through the TiC_x layer. The whole process can be described: C atoms diffusing through the TiC_x layer dissolved into the Ni–Ti liquid and TiC were formed once the liquid became supersaturated. Simultaneously, the heat generated from the TiC formation made the unstable TiC_x layer break up. However, with the spread of Ti–Ni liquid, a new TiC_x layer was formed again at the interface between spreading liquid and C particle. This process cannot stop until all the C particles are consumed completely.

1. Introduction

The characteristics of extremely fast heating and high temperature in the self-propagating high-temperature synthesis (SHS) made it potential to produce materials with novel structures and properties, including ceramics, ceramic matrix composites, nanophase materials and intermetallics [1,2]. Among these materials, TiC, as a typical one of these ceramics, was paid more attention due to its low density and chemical reactivity, as well as its high hardness, good elastic modulus and high melting temperature [3].

TiC can be produced from mixtures of titanium and carbon powders by SHS. Generally, the formation of liquid and its subsequent capillary spreading are essential to the ignition and propagation of the combustion wave. However, the ignition temperature for Ti–C binary system is very high and even close to the melting point of titanium. Therefore, those second metals with low melting point are introduced to decrease the ignition temperature by forming low-melting intermetallics and evolving into a liquid at a low temperature (eutectic temperature) to improve the mass transference [4–18]. On the other hand, the fracture toughness of a TiC composite can also be improved by adding a ductile metal as a continuous phase. Among these metals, the liquid Ni form with solid TiC for the low wetting angle under vacuum at 1450 °C [19]. This makes Ni be selected as the additive metal, which can not only promote the easy occurrence of the SHS reaction, but also improve the structural applications.

However, reports on SHS reaction mechanism in the Ni–Ti–C system are very controversial. In general, the mechanism about the formation of TiC can be confirmed to be dissolution, reaction and precipitation. Nevertheless, two mechanisms about the formation of the liquid exist: one is the prior formation of Ti_2Ni formed by the solid reaction and then the formation of Ni–Ti liquid over the eutectic temperature between Ti_2Ni and Ti, which has been supported by Dunmead et al. [7], Xiao et al. [3] and Lasalvia et al. [8,9]; the other is the formation of Ti liquid caused by the direct melting of Ti during the SHS reaction, which has been suggested by Wong et al. [18]. Thus it can be seen, there is a general lack of consistency in the SHS mechanism for Ni–Ti–C system, and no firm understanding are agreed. Moreover, it is important to notice that the sizes of C particles used in the aforementioned literatures are very fine, such as carbon black and furnace black. Actually, in our previous study [20], the C particle size had a profound influence on the ignition and combustion characteristics of the SHS reaction in the 20 wt.% Ni–Ti–C system. Consequently, it can be believed to influence the SHS mechanism of the Ni–Ti–C system as well.

Therefore, the purpose of the present study is to clarify the formation mechanism of liquid and investigate the effect of C particle size on the SHS mechanism of the Ni–Ti–C system. The apparent activation energies of the SHS reactions in the Ni–Ti–C system with fine and coarse C particles are estimated to speculate the SHS mechanism by measuring the combustion temperature and wave velocity. In particular, in the Ni–Ti–C system with coarse C

* Corresponding authors. Tel.: +86 431 8509 4699; fax: +86 431 8509 4699.
E-mail addresses: y.yang6@uq.edu.au (Y.F. Yang), jqc@jlu.edu.cn (Q.C. Jiang).

0925-8388/$ – see front matter © 2011 Elsevier B.V. All rights reserved.
doi:10.1016/j.jallcom.2011.03.165

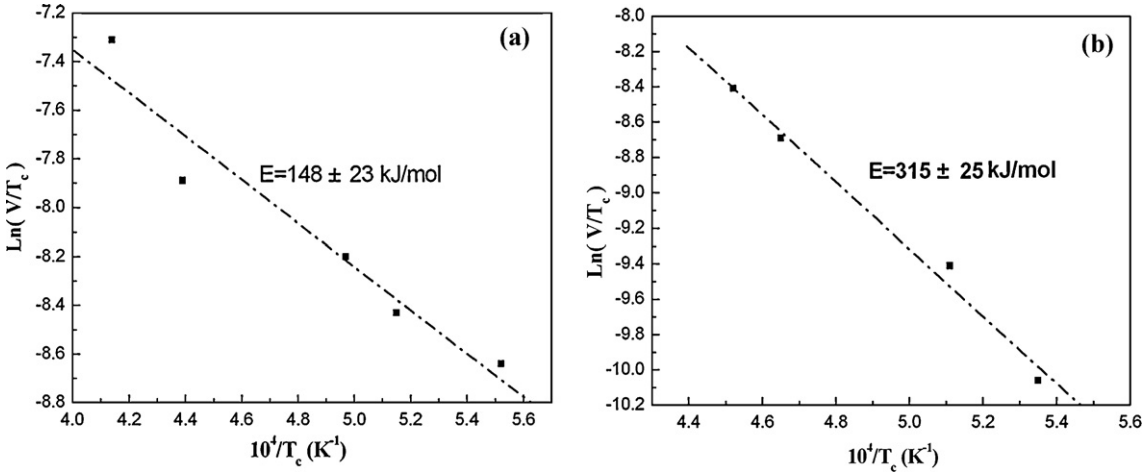

Fig. 1. Arrhenius plot of $\mathrm{Ln}(V/T_c)$ vs. $1/T_c$ for the SHS reaction in the Ni–Ti–C system with (a) ~1 μm and (b) ~48 μm C particles.

particle, a detailed phase transformation sequence and a delicate microstructure evolution during the passage of combustion wave are addressed to prove the speculated mechanism. It is expected that these results can be significant in effectively controlling the SHS process and promoting the use of TiC/Ni composites in practice.

2. Experimental

The starting materials were made from commercial powders of Ni (99.5% purity) with an average particle size of ~45 μm, TiC (98% purity) with an average particle size of ~48 μm, Ti (99.5% purity) with an average particle size of ~25 μm and C (99.5% purity), where two kinds of C particle sizes (with an average particle size of ~38 μm and ~1 μm, respectively) were selected.

Reactant powder mixtures were prepared for the following basic reaction:

$$\mathrm{Ti} + \mathrm{C} + 30\,\mathrm{wt.\%Ni} = \mathrm{TiC} + 30\,\mathrm{wt.\%Ni} \quad (1)$$

The combustion temperatures were varied by controlling the addition of TiC powder which acted as an inert diluent. The reactant powders were weighed out in the proper stoichiometric proportions, keeping a constant equimolar ratio of Ti and C, but varying the amount of Ni and TiC. Three kinds of hardened steel grinding ball (1.5, 1.0 and 0.5 cm in diameter) were used as milled balls, and the amount ratio of three kinds of balls were the same. After being sufficiently dry-mixed by mechanical stirring at 25 rpm for 8 h without any liquid medium, the blends were uniaxially pressed into cylindrical preforms (20 mm diameter) under pressures to obtain green densities of 75 ± 2% theoretical density.

Details of the experimental apparatus and procedure for the SHS reaction were given in a previous article [20]. The combustion wave velocities were measured by recording the whole combustion event with a white-black CCD video camera (DALSA) at 45 frames per second. The combustion temperatures were achieved using a thermocouple pair of W–5%Re vs. W–26%Re (0.5 mm in diameter) at the centre of the perform, where the measured temperature lags 1.5 s behind the real temperature. In order to make clear the reaction sequence and phase formation mechanism in the Ni–Ti–C system with coarse C particle, the combustion wave was quenched during its passage through the sample. A long and thin rectangular sample (65 mm × 14 mm × 6 mm) favors the combustion extinguishing in the halfway by increasing heat loss and reducing heat production. In the present study, the combustion front could be made to stop by sandwiching a part of the sample between two copper plates. The quenched sample was polished and etched for phase analysis and microstructure evolution characterization. The phase constituents in the differently reacted regions were identified by the X-ray microdiffractometer (D8 Discover with GADDS, Bruker AXS, Germany) using the 800 μm beam diameter. The microstructures were investigated by using scanning electron microscopy (SEM) (Model JSM-5310, Japan) equipped with energy-dispersive spectrometer (EDS) (Model Link-ISIS, Britain).

3. Results

The propagation wave velocity and the combustion temperature can be related by Merzhanov equation [21]:

$$V^2 = \sigma_n \alpha \frac{C_p}{Q} \frac{RT_c^2}{E} k_0 \ \exp\left(\frac{-E}{RT_c}\right) \quad (2)$$

where V is the wave velocity, α is the thermal diffusivity, σ_n is a constant which depends upon the order of the reaction, T_c is the combustion temperature, and R is the gas constant, C_p and k_0 are the heat capacity and the thermal conductivity, Q is the heat of the reaction and E is the activation energy. Eq. (2) can also be expressed by:

$$2\ \mathrm{Ln}\left(\frac{V}{T_c}\right) = \mathrm{Ln}\left(\sigma_n \alpha \frac{C_p}{Q} \frac{R}{E} k_0\right) - \frac{E}{RT_c} \quad (3)$$

It should be noted that the thermophysical and thermochemical properties of both reactants and products are assumed to be invariable in the present calculation. Therefore, the $\mathrm{Ln}(V/T_c)$ exhibits a line function as $1/T_c$, and the slope is $-E/R$. The apparent activation energies of the SHS reaction can be determined from the Arrhenius plot of $\mathrm{Ln}(V/T_c)$ vs. $1/T_c$, and it can be calculated according to the slope. To do this, the propagation velocity and combustion temperature should be varied. This can be accomplished by adding inert phase as a diluent into the reactants. However, different starting compositions used in different experiments imply that in each experiment these parameters such as specific heat, thermal diffusivity, thermal conductivity, and most importantly, reaction heat and activation energy are different. Lakshmikantha and Sekhar [22] developed an improved kinetic equation by considering the differences of heat capacity, thermal conductivity, and density for reactants and products as well as dilution effect. The modified kinetic equation indicated that it affected only the pre-exponential factor. For the purpose of activation energies determination, the results were the same. Moreover, assuming that $\mathrm{Ln}(\sigma_n \alpha (C_p/Q)(R/E)k_0)$ was a constant, we found that the $\mathrm{Ln}(V/T_c)$ indeed exhibited a line function as $1/T_c$, as shown in Fig. 1, which suggests that these changes caused by different starting compositions may not influence the apparent activation energies greatly. The same method as that in the present study has been widely used for activation energies determination in many literatures [7,22–25].

The combustion parameters measured in the Ni–Ti–C system with ~1 μm C particle are listed in Table 1 and are plotted in Arrhenius form in Fig. 1(a). Using the slope of the line, the apparent activation energy is determined to be 148 ± 23 kJ/mol. The combustion parameters measured in the Ni–Ti–C system with ~48 μm C particle are listed in Table 2 and are plotted in Arrhenius form in Fig. 1(b). It is worth noting that when the TiC powder with 15 wt.% was added, the SHS reaction cannot be initiated successfully. Using the slope of the line, the apparent activation energy was determined to be 315 ± 25 kJ/mol.

Table 1
Experimental combustion parameters for the Ni–Ti–C system with fine C particle.

Ni content (wt.%)	TiC content (wt.%)	Combustion temperature (K)	Wave velocity (cm/s)
30	0	2412	1.0625
30	3	2279	0.855
30	6	2010	0.55
30	11	1940	0.42
30	15	1810	0.32

In order to validate the mechanism, the combustion wave was quenched during its passage through the sample to make clear the reaction sequence and phase formation mechanism. Due to the considerable similarity in the microstructure evolution of the quenched samples from the 30 wt.% Ni–Ti–C systems (without TiC dilution and with 6 wt.% TiC dilution) with coarse C particle, only the quenched sample from the 30 wt.% Ni–Ti–C system (without TiC dilution) with coarse C particle was discussed in the manuscript. Depending upon the extent of reaction, the sample can be divided into four distinct regions, i.e., (1) unreacted regions, (2) preheated region, (3) combustion region and (4) fully reacted region. And there are well-defined boundaries among these four regions. A detailed phase constituent analysis of the different regions was carried out in a combustion-wave quenched sample with coarse C particle, as shown in Fig. 2. The microstructure evolution during SHS process were achieved by the microstructure observation and EDS analysis of the different regions in a combustion-wave quenched sample, and the detailed results are shown in Figs. 3 and 4, respectively.

4. Discussion

4.1. Theory analysis

For the fine C particle, the apparent activation energy for the formation mechanism of TiC is determined to be 148 ± 23 kJ/mol. No literature data could be found for the activation energy of the dissolution of C into a Ni–Ti melt. Dunmead et al. [7] concluded that the formation mechanism of TiC was a mechanism of the dissolution of C into the Ni–Ti liquids and precipitation of TiC from the supersaturated liquids, according to the comparison that the apparent energy (133 ± 50 kJ/mol) measured in their study is close to that (117 kJ/mol [26]) of dissolution of C into liquid Ti. It can be seen, however, that the activation energy (148 ± 23 kJ/mol) for this process with fine C particle in the present study is very similar to that of Dunmead's. Therefore, a comparison of these values indicates that the formation of TiC from the system with fine C particle in the present study is controlled by a mechanism of dissolution and precipitation. This means that fine C particle can dissolve into the Ni–Ti liquids and TiC can form and precipitate out of the supersaturated Ni–Ti–C liquids. The existence of this dissolution and precipitation mechanism in the Ni–Ti–C system has been further substantiated by the microstructure evolution observation in the quenched sample [3]. Oppositely, for the coarse C particle, the apparent activation energy for the formation mechanism of TiC is determined to be

Table 2
Experimental combustion parameters for the Ni–Ti–C system with coarse C particle.

Ni content (wt.%)	TiC content (wt.%)	Combustion temperature (K)	Wave velocity (cm/s)
30	0	2210	0.49
30	3	2150	0.36
30	6	1956	0.16
30	11	1870	0.08
30	15	–	–

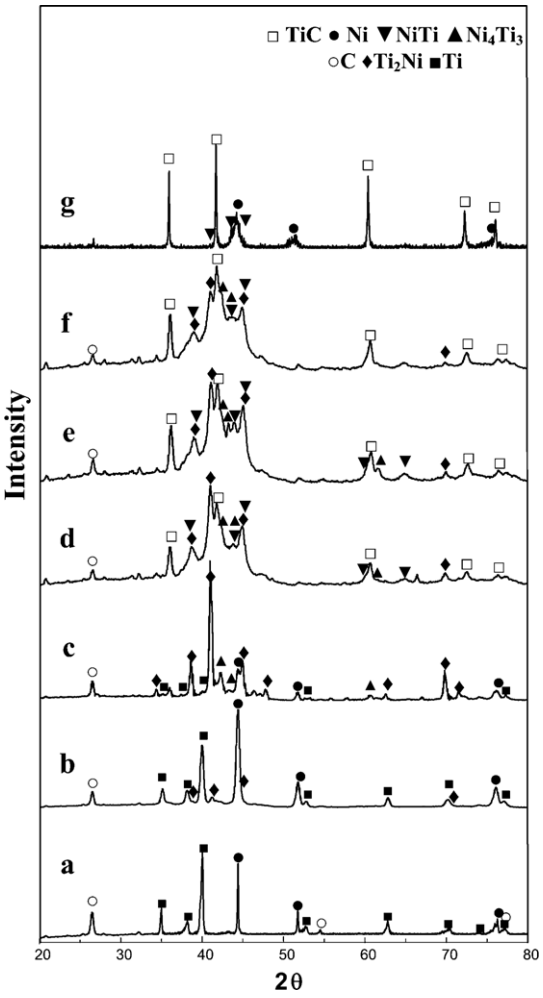

Fig. 2. X-ray microdiffractometer results of the phase constituents in the different combustion zones: (a) unreacted region; (b) the boundary between the unreacted region and preheated region; (c) the preheating region; (d) the boundary between the preheated region and combustion region; (e) the combustion region; (f) the boundary between the fully reacted region and combustion region; (g) the fully reacted region.

315 ± 25 kJ/mol. It was reported that the activation energy for the diffusion of C through solid TiC was approximately in the range of 347–410 kJ/mol [27–29]. The calculated value in the present study is a little lower than the reported activation energy for the diffusion of C through TiC, but much lower than that (~738 kJ/mol [28]) of the diffusion of Ti through TiC. This comparison suggests that the formation of TiC from the system with coarse C particle may be controlled by the diffusion of C through TiC_x layer. This implies that the formation of TiC in the Ni–Ti–C system with ~48 μm C particle may occur via a carburization process, where a TiC_x layer firstly forms around the C particle and most of C atoms have to diffuse through the product layer to further form TiC. Nevertheless, it is important to notice that it is a theory speculation and is insufficient to determine the SHS mechanism if only from the comparison of the activation energy value. Therefore, an analysis about the microstructure evolution in the quenched sample during SHS reaction is carried out to validate the SHS mechanism.

4.2. Phase constituents of different regions

Fig. 2 shows the X-ray microdiffractometer results of the phase constituents in the different regions. As indicated in Fig. 2(a), the phases in the unreacted region are composed of Ni, Ti and C. The sec-

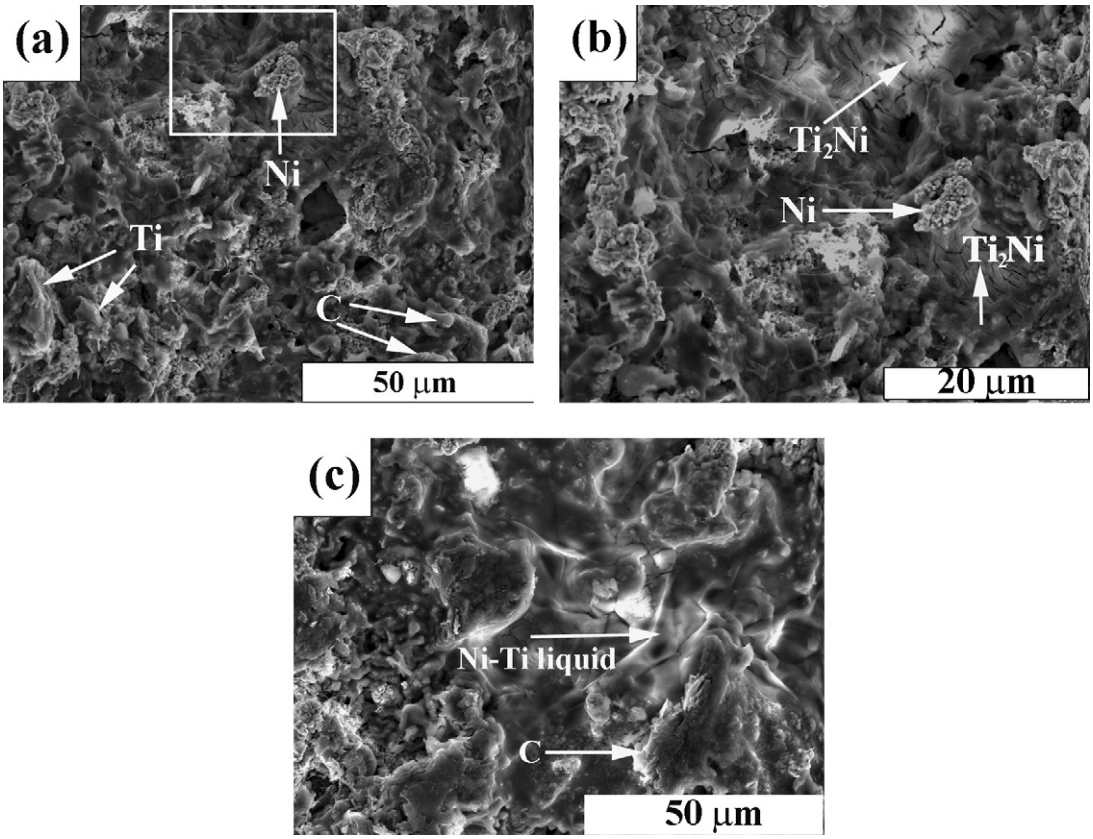

Fig. 3. (a) The representative microstructures at the centre of the preheated region, (b) the magnified microstructures of the marked region in (a), and (c) the microstructure of the interface between the preheated and *t* combustion regions.

ond spot is chosen at the boundary between the unreacted region and preheated region. XRD results show that a few Ti_2Ni appear in the products at the boundary, besides unreacted Ni, Ti and C, as shown in Fig. 2(b), which suggests that the solid diffusion reaction firstly occurs between Ni and Ti. The third spot is chosen at the centre of the preheating region. The products at this position consist of a large number of Ti_2Ni, a few Ni_4Ti_3 and unreacted Ti, as shown in Fig. 2(c), which suggests that the main reactions occurred in the preheated region correspond to the formation of Ni–Ti intermediate phases. In addition, the intensity of Ti_2Ni increases greatly, compared with that in the second spot. Fig. 2(d) indicates the XRD patterns of the products at the boundary between the preheated and combustion regions. As can be seen, a few TiC are detected in the products at this position, besides a large number of Ti_2Ni and a few NiTi and Ni_4Ti_3. Actually, the Ni–Ti liquid over the eutectic temperature between Ti_2Ni and Ti could be formed at this region according to the Ni–Ti phase diagram [30], which can be clearly observed in the microstructural evolution in the latter paragraph. Therefore, some of Ni–Ti compounds are formed during the solidification. Fig. 2(e) indicates the XRD patterns of the products in the combustion region. As indicated, the amount of TiC is much higher than that in the fourth spot, but numerous Ni–Ti phases can still be detected in this region, which suggests that the SHS reaction is being in progress. The sixth spot is chosen at the boundary between the combustion region and fully reacted region. Compared with the XRD results in the combustion region, the intensity of TiC increases while those of Ni–Ti intermediate phases decrease, as shown in Fig. 2(f), which suggests that the main reaction occurred in this region corresponds to the formation of TiC ceramic. Fig. 2(g) shows the XRD results of the fully reacted region. It can be observed that the final products only consist of TiC and Ni with only a small amount of NiTi intermediate phases, which indicates that the SHS reaction is nearly complete.

Despite the fact that some phases might be omitted due to the limitation of examination spots, a general plot of the SHS reaction mechanism in the Ni–Ti–C system can be established. The reaction sequence can be described as: (1) $Ni + Ti + C \rightarrow$ (2) $Ti_2Ni + Ni + Ti + C \rightarrow$ (3) $Ti_2Ni + Ni_4Ti_3 + Ti + Ni + C \rightarrow$ (4) the formation of Ni–Ti liquids $\rightarrow$ (5) the formation and precipitation of TiC.

4.3. Microstructural evolution

At the unreacted region, C particles are surrounded closely by the Ni and Ti particles which touch with each other very well. Fig. 3(a) shows the representative microstructure at the centre of the preheated region. XRD results on this region indicate that the phases consist of a large number of Ti_2Ni and a few Ni_4Ti_3, as well as some unreacted Ni, Ti and C. As can be seen in Fig. 3(a), numerous Ni–Ti phases which are different from individual Ni and Ti particles morphologically can be observed. In addition, some unreacted Ni, Ti and C particles are surrounded by these Ni–Ti intermediate phases. However, the Ti_2Ni and Ni_4Ti_3 phases cannot be readily distinguished from the SEM photograph. Fig. 3(b) presents the magnified microstructures of the marked region in Fig. 3(a). It can be clearly observed that the Ni particle is being consumed by forming Ni–Ti intermediate phases. EDS results indicate the average Ni/Ti atomic ratio in these intermediate phases is about 38:62, close to the composition of Ti_2Ni, which suggests that the solid reaction between Ni and Ti firstly occurs to form Ti_2Ni, as shown in Fig. 3(b). The aforementioned results suggest that although the reaction formed TiC between Ti and C cannot be progressed at this stage due to diffusion limitation despite that it possesses lower ΔG° [31].

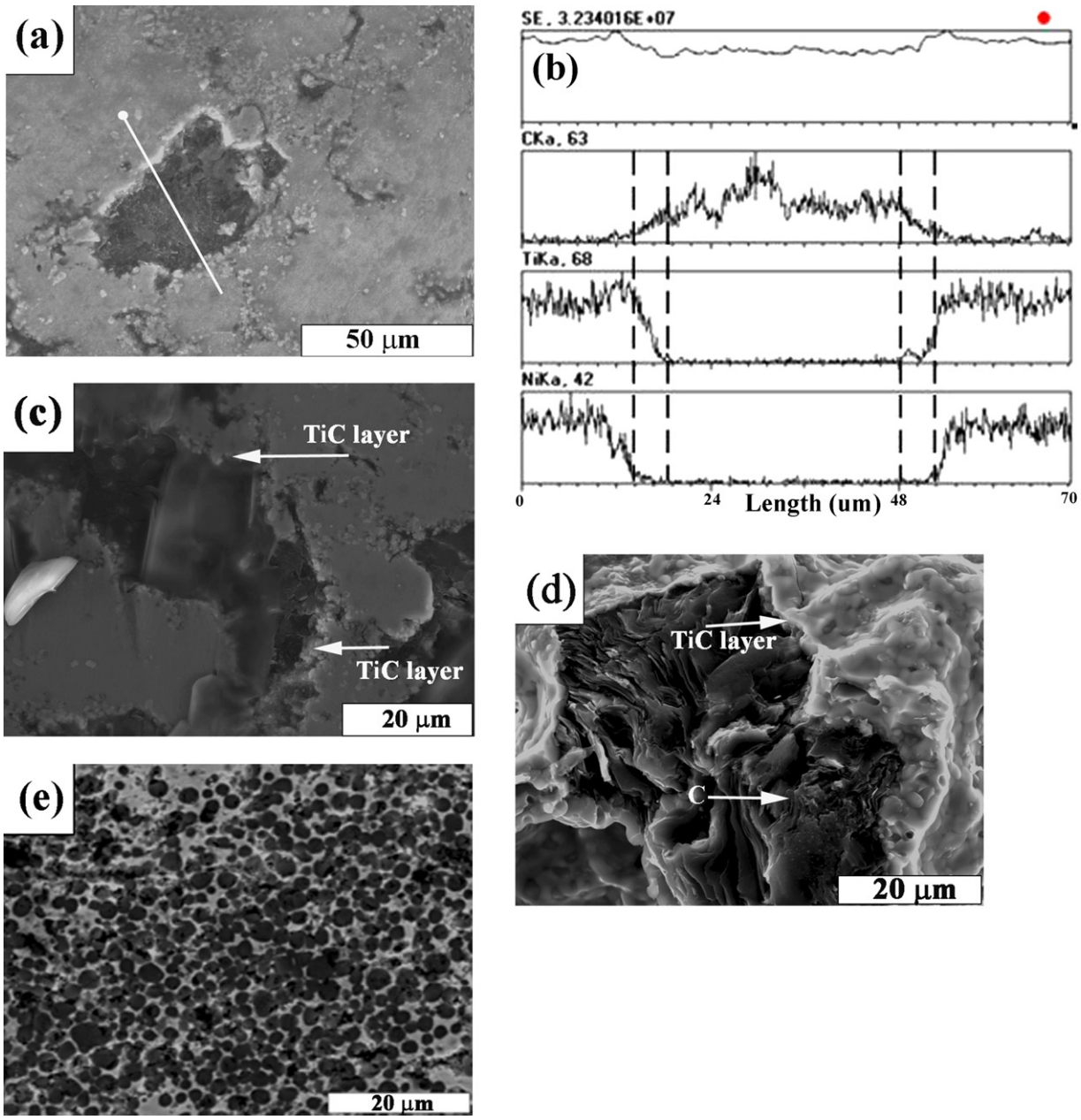

Fig. 4. (a) The typical microstructures, (b) EDS-line analysis at the centre of the combustion region, (c) and (d) the magnified morphologies of TiC_x layer formed around C particles and (e) the typical microstructure of the fully reacted region.

Fig. 3(c) shows the typical micrograph of the interface between the preheated and combustion regions. The development of Ni–Ti compounds can advance the liquid formation since the eutectic temperatures between Ni–Ti intermetallic compounds and Ti are much lower than the melting points of Ti, Ni and C. As a consequence, some Ni–Ti liquids begin to appear at this stage, as can be seen in Fig. 3(c). XRD results on this position indicate the products mainly consist of a few TiC, Ti_2Ni, Ni_4Ti_3 and NiTi during solidification, as well as unreacted C. In fact, the formation of these Ni–Ti liquid phases is of vital importance since it greatly improves their contact with the C particle and reduces the atomic diffusion distance for the subsequent reaction. Once formed, the Ni–Ti liquids will spread and surround the C particle, which led to a significant increase in the contact area between Ti and C particle. Subsequently, the reactions between Ti and C can occur to form TiC_x layer around the C particle, as will be discussed in the latter paragraph.

Fig. 4(a) exhibits the representative microstructure at the centre of the combustion region. It can be observed that the C particle is surrounded by the Ni–Ti liquids. In order to verify whether the TiC_x layer exists or not, the EDS-line analysis is carried out and the results are shown in Fig. 4(b). As indicated, relatively high concentration of Ti and C simultaneously distribute around the C particle, and there is a long distance along the line where both Ti and C distribute largely, as marked in Fig. 4(b), which suggests that the TiC_x layer does form and exist around the C particle. Fig. 4(c) and (d) indicates the magnified morphologies of TiC_x layer formed around C particle. Obviously, some nearly spherical fine TiC particulates distribute around the C particle, and just these particulates construct into the TiC_x layer. Nevertheless, a few Ni liquid are displaced together with the formation of TiC_x layer and reside among the gap in the TiC_x layer. Just these Ni liquids provide an easy route for the transfer between Ti and C. Due to the higher diffusivity of C (compared with Ti), C atoms on the surface of remnant C particle can

dissolve into the Ni liquid. With the help of Ni liquid, these C atoms easily diffuse through the TiC_x layer into the Ni–Ti liquids to form Ni–Ti–C liquids, and TiC precipitates out of the liquids once the Ni–Ti–C liquids become supersaturated. Actually, with the help of Ni liquid, it is easier for this process in the present study to occur, compared with that of the diffusion of C through solid TiC in the reported results [27–29]. Therefore, the apparent activity energy in the present study is a little lower than those reported values. Generally, the stoichiometry (x) of TiC_x layer is much lower than 1.0 due to the participation of fewer C atoms, and therefore the breaking temperature of unstable TiC_x layer is relatively low according to the phase diagram [30]. Subsequently, the heat generated from the forming TiC reaction that C atoms diffusing through the TiC layer dissolve into the Ni–Ti liquid to form TiC can make the unstable TiC_x layer break up easily. After that, the new TiC_x layer can be formed between the spreading Ni–Ti liquids and C particle. This process corresponding to the breaking up of the primary TiC_x layer and subsequent formation of the new TiC_x layer cannot stop until all the C particles are consumed completely. And the final products consist of large numbers of TiC particles without residual C particle, as shown in Fig. 4(e).

On the basis of the calculation of activation energy and the above observation made in this study, the SHS reaction mechanism of the Ni–Ti–C system with the coarse C particle can be determined to be a mechanism of the diffusion of C through the TiC_x layer with the help of the Ni liquid. Actually, the great disparity about the SHS mechanism in the Ni–Ti–C system with different C particles can be attributed to the difference in the size of C particles. The fine C particle leads to an increase in the contacting area between Ni–Ti liquids and C particle, which can improve the surface reaction rate greatly. In addition, it is much easier and quicker for fine C particle to dissolve into Ni–Ti liquids completely, compared with the coarse C particle. Therefore, the Ni–Ti–C liquids can be formed quickly during a shorter time. And further, the reaction of forming TiC occurs fast, which is consistent with our previous study where only one combustion wave was found [20]. In contrary, it is relatively difficult for the coarse C particle to dissolve into the Ni–Ti liquids quickly and completely. On the other hand, the coarse C particle can lead to the decrease in the contacting area between Ni–Ti liquids and C particle. Nevertheless, some reactions forming TiC can occur firstly due to the relatively high activity of C atoms on the surface of the coarse C particle, which contributes to the formation of TiC_x layer around the coarse C particle. Most of the other C atoms have to diffuse through the TiC_x layer into the Ni–Ti liquids to form TiC. Therefore, the formation rate of TiC is lowered significantly and two different combustion waves were found in our previous study [20], where the first wave corresponded to the formation of Ti_2Ni and the second one was the formation of large numbers of TiC. In addition, due to the low reaction rate compared with fine C particle, the combustion temperature was much lower than fine C particles.

5. Conclusion

- The liquid firstly formed in Ni–Ti–C system should be Ti–Ni liquid which evolved from the eutectic reaction between Ti_2Ni and Ti, regardless of coarse or fine C particle.
- Two different mechanisms domain the formation of TiC with coarse and fine C particles. For the fine C particle, the formation of TiC is controlled by a mechanism of dissolution, reaction and precipitation. For the coarse C particle, a TiC_x layer can be formed firstly and the formation of TiC is controlled by a mechanism of the diffusion of C through a TiC_x layer with the help of the Ni liquid.
- The reaction pathway for the coarse C particles can be described as: (1) $Ni + Ti + C \rightarrow$ (2) $Ti_2Ni + Ni + Ti + C \rightarrow$ (3) $Ti_2Ni + Ni_4Ti_3 + Ti + Ni + C \rightarrow$ (4) the Ni–Ti liquids over the eutectic temperature between Ti_2Ni and $Ti \rightarrow$ (5) the formation of TiC_x layer $\rightarrow$ (6) the diffusion of C through the TiC_x layer to form the supersaturated Ni–Ti–C liquids with the help of Ni liquid $\rightarrow$ (7) formation and precipitation of TiC. The heat generated from the forming TiC reaction can make the unstable TiC_x layer break up. However, the new TiC_x layer can be formed again at the interface between the spreading liquid and C particle. The process cannot stop until all the C particles are consumed completely.

Acknowledgements

This work is supported by NNSFC (No. 50531030), MSTC (Nos. 2006AA03Z566 and 2005CCA00300) and NCET (No. 06-0308) as well as The Project 985-Automotive Engineering of Jilin University.

References

[1] S.C. Tjong, Z.Y. Ma, Mater. Sci. Eng. R. 29 (2000) 49–113.
[2] C.L. Yeh, W.Y. Sung, J. Alloy Compd. 376 (2004) 79–88.
[3] G.Q. Xiao, Q.C. Fan, M.Z. Gu, Z.H. Wang, Z.H. Jin, Mater. Sci. Eng. A 382 (2004) 132–140.
[4] Y. Choi, J.K. Lee, M.E. Mullins, J. Mater. Sci. 32 (1997) 1717–1724.
[5] A. Saidi, A. Chrysanthou, J.V. Wood, J.L.F. Kellie, J. Mater. Sci. 29 (1994) 4993–5000.
[6] Q.C. Fan, H.F. Chai, Z.H. Jin, J. Mater. Sci. 32 (1997) 4319–4323.
[7] S.D. Dunmead, D.W. Ready, C.E. Semler, J.B. Holt, J. Am. Ceram. Soc. 72 (1989) 2318–2324.
[8] J.C. LaSalvia, D.K. Kim, R.A. Lipsett, M.A. Meyers, Metall. Mater. Trans. A 26A (1995) 3001–3010.
[9] J.C. LaSalvia, M.A. Meyers, Metall. Mater. Trans. A 26A (1995) 3011–3019.
[10] H.J. Brinkman, J. Zupanic, J. Duszczyk, J.L. Katgerman, J. Mater. Res. 15 (2000) 2620–2627.
[11] I. Gotman, M.J. Koczak, Mater. Sci. Eng. A 187 (1994) 189–199.
[12] W.C. Lee, S.L. Chung, J. Am. Ceram. Soc. 80 (1997) 53–61.
[13] X.H. Zhang, J.C. Han, S.Y. Du, J.V. Wood, J. Mater. Sci. 35 (2000) 1925–1930.
[14] I.J. Shon, Z.A. Munir, J. Am. Ceram. Soc. 81 (1998) 3243–3248.
[15] J.C. Han, X.H. Zhang, J.V. Wood, Mater. Sci. Eng. A 280 (2000) 328–333.
[16] Z.A. Munir, Am. Ceram. Soc. Bull. 67 (1988) 342–349.
[17] S.K. Mishra, S.K. Das, A.K. Ray, P. Ramchandrarao, J. Mater. Res. 14 (1999) 3594–3598.
[18] J. Wong, E.M. Larson, J.B. Holt, P.A. Waide, B. Rupp, R. Frahm, Science 249 (1990) 1406–1409.
[19] N. Durlu, J. Eur. Ceram. Soc. 19 (1999) 2415–2419.
[20] Y.F. Yang, H.Y. Wang, Y.H. Liang, R.Y. Zhao, Q.C. Jiang, J. Alloy Compd. 460 (2008) 276–282.
[21] A.G. Merzhanov, Combust. Flame 13 (1969) 143–147.
[22] M.G. Lakshmikantha, J.A. Sekhar, J. Am. Ceram. Soc. 77 (1994) 202–210.
[23] M. Fu, J. Mater. Res. 12 (1996) 1481–1491.
[24] Z.Y. Fu, H. Wang, W.M. Wang, R.Z. Yuan, J. Mater. Process. Technol. 137 (2003) 30–34.
[25] J.B. Holt, Z.A. Munir, J. Mater. Sci. 21 (1986) 251–259.
[26] A.I. Kirdyashkin, Yu.M. Maksimov, E.A. Nekrasov, Combust. Explos. Shock Waves 17 (1981) 377–379 (Engl. Transl.).
[27] S. Sarin, J. Appl. Phys. 39 (1968) 3305–3310.
[28] S. Sarin, J. Appl. Phys. 39 (1968) 5036–5041.
[29] D.L. Kohlstedt, W.S. Williams, J.B. Woodhouse, J. Appl. Phys. 41 (1970) 4476–4484.
[30] T.B. Massalski, H. Okamoto, P.R. Subramanian, L. Kacprzak, Binary Alloy Phase Diagrams, 2nd ed., ASM International, Materials Park, OH, 1990.
[31] I. Barin, Thermochemical Data of Pure Substances, 2nd ed., VCH GmbH, Weinheim, Germany, 1993.